Solid State Phenomena
ISSN: 1662-9779, Vol. 214, pp 58-66
doi:10.4028/www.scientific.net/SSP.214.58

Online: 2014-02-27

Comparison of Electromagnetic Coil Launcher Model with Real-Device Characteristics

Mirosław Kondratiuk[1, a], Zdzisław Gosiewski[1,b]

[1]Bialystok University of Technology, Mechanical Faculty,

Department of Automatics and Robotics,

Wiejska St. 45C, 15-351 Bialystok, Poland

[a]m.kondratiuk@pb.edu.pl (corresponding author), [b]z.gosiewski@pb.edu.pl

Keywords: coil launcher, unmanned aerial vehicles catapult, electromagnetic launcher, finite element method in magnetic calculations,

Abstract. In this paper we describe a numerical model and a construction of an electromagnetic launcher (EML) consisting of ten copper coils located serially. The solenoids were mounted on the pipe-shaped slideway, inside which the ferromagnetic core was moved driven by the coils' magnetic force. The paper presents the model of an EML based on circuit approach involving lumped parameters which were obtained by means of a finite element methods (FEM). The numerical representation contained a mechanical part with introduced friction coefficients. In the article we proposed an algorithm which enabled us to fit the numerical model to the constructed device by selection of these friction parameters values. Thus, we were able to compare the signals from computer simulations and measurements which were taken during laboratory tests.

Introduction

The research on the electromagnetic launchers (EMLs) for micro aerial vehicles (MAVs) has been conducted at the Bialystok University of Technology since 2007, [1, 2, 3]. The research concerns numerical calculations and their practical applications. Magnetic launchers for MAVs can be an alternative to presently used solutions which employ rubber or compressed air drives. Catapults based on electromagnetic phenomena have a significant advantage over the classical launchers mentioned above, namely, they enabled us to control launch force and acceleration of the starting vehicles. It is especially important when operated microplanes (of mass up to 5 kg) are equipped with calibrated devices such as autopilots, inertial measurement units (IMUs) or other fragile sensors which should not be maladjusted during assisted take-offs. It is particularly essential in applications connected with UAVs formation flight control where employment of a magnetic launcher with controlled acceleration could significantly increase an autonomy and reliability of such system [4, 5]. Another advantage of EMLs is that the nomenclature and the way of modelling of such devices can be very similar to linear motors which for instance, can be seen in [6, 7, 8].

Construction of the coil launcher

Out of two main types of electromagnetic launchers (involving rail or coil technology [9, 10]) we chose the one based on solenoids. This choice was dictated by simplicity of construction, modularity of the construction and, what is the most important, by the possibility controlling the magnetic force. Our design involved 10 serially located air coils with cylindrical ferromagnetic core moving inside (coils can be called "drive-modules"). The core was connected by the diamagnetic pusher to the car. In order to minimize buckling, the pusher was composed of brass wire core and cylindrical carbon shield. On this car a launched object was mounted. In the electrical circuit of each coil Hall sensors (LEM CAS 25-NP) were installed. It enabled us to measure currents flowing through the coils wires in order to use their values in control operations. The positions of the core and the launched object were precisely obtained by means of resistive transducer (Megatron MSL38 E)

which was an integral part of the launcher construction. During launches, the main signal in the feedback control loop was MAV's take-off acceleration. It was measured by a micro electromechanical accelerometer (MMA7260Q) with a maximum range of ± 60 m/s^2. The sensor was fixed to the car so that its indications were directly translated into ferromagnetic core acceleration (buckling of the pusher was negligibly small). The scheme of the 10-coil launcher was presented in Fig. 1. The construction of the launcher laboratory stand was described in greater detail in previous papers [11, 12].

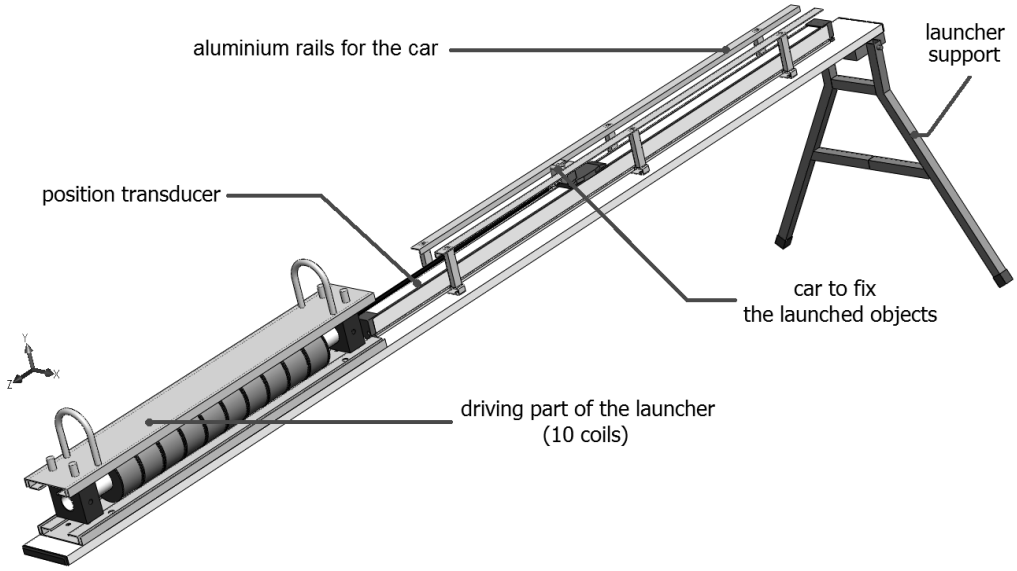

Fig. 1. Computer aided design (CAD) representation of the electromagnetic coil launcher construction

In the process of design we used numerical models based only on finite element methods (FEM). Before we started to build the launcher, we tried to obtain the best possible drive-modules turns configuration. We were looking for such solenoid parameters which provided the greatest possible increase of the core velocity in the shortest time period. Obtained results and description of numerical research were specified in detail in our paper [12].

In this article we focused on the employed methods of core motion modelling in our FEM calculations.

Calculations based on FEM

The design of the launcher required developing the numerical model of a single drive-module with a ferromagnetic core. Dimensions of the core, magnetic characteristics of the ferromagnetic material and coil wire parameters were known from technical specifications and data sheets. Thus, we could focus only on the selection of the coil turns configuration.

In the model we used a time-dependent solver which means that we had to solve a system of field equations of the general form:

$$\sigma\frac{\partial \mathbf{A}}{\partial t}+\nabla\times\frac{\mathbf{B}}{\mu_0\mu_r(\mathbf{B})}-\sigma\mathbf{v}\times\mathbf{B}=\mathbf{J}_e. \tag{1}$$

$$\mathbf{B}=\nabla\times\mathbf{A}. \tag{2}$$

where: σ – electric conductivity, [S/m]; **A** – magnetic field vector potential, [Wb/m]; **B** – magnetic flux density, [T]; μ_0 – permeability of vacuum, [H/m]; $\mu_r(\mathbf{B})$ – relative permeability (dimensionless); **v** – vector of linear velocity, [m/s]; $\mathbf{J}_e$ – vector of external current density, [A/m^2].

More details about transformations of Ampere's equation from general form into axial symmetry form can be found in [13].

In calculations we employed a ready-made FEM package - COMSOL Multiphysics - with AC/DC Module, [14]. This software provided a few methods which enabled the users to conduct calculations for objects moving in the magnetic field. In most cases the technique called *moving mesh* could be applied. It based on the mesh nodes displacement computed from previously defined ordinary differential equation (ODE) of motion. In our case the ODE took the following form:

$$\frac{\mathrm{d}^2 z}{\mathrm{d}t^2} = \frac{F_m}{m_c + m_o}. \tag{3}$$

where: z – core (and launching object) displacement, [m]; F_m – magnetic force, [N]; m_c, m_o – core and object mass, respectively, [kg].

Magnetic force was calculated by Maxwell's stress tensor approach. Computations were carried out on DELL Precisions 7400 work station. The device was equipped with 8 Intel Xeon 3.2 GHz processors, 16 GB of memory (RAM) and MS Windows 7 operating system. Areas of the mesh densities and rarefactions for employed *moving mesh* technique in the axis symmetric time-dependent model were shown in Fig. 2.

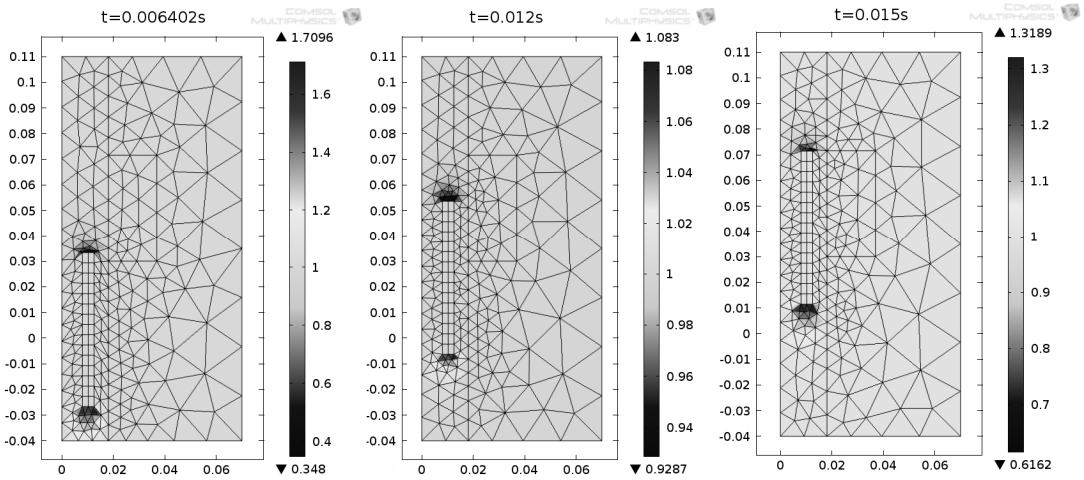

Fig. 2. Areas of the finite element mesh densities and rarefactions for axis symmetric time dependent model

It is worth mentioning that in calculations conducted by means of COMSOL an extra utility was used, namely, a *remeshing* technique. It is based on reconfiguration of deformed mesh elements under the qualifications defined by the user. As the remeshing condition we chose the mesh quality parameter that varied from 0 to 1 where 0 and 1 denoted poor and perfect mesh qualities respectively.

The second approach to motion modelling provided by COMSOL was the *Euler's method*. That technique based of constant mesh distribution in the investigated system in special way, which enabled us to describe the moving part (core) as functional variation of material parameters. In our case these parameters were relative permeability (μ_r) and conductivity (σ) of the ferromagnetic material. In the model, instead of μ_r and σ coefficients, we introduced γ_μ and γ_σ functions which corresponded to above mentioned parameters. Their equations had the following forms:

$$\gamma_\mu(r,z,t) = \xi(z) \cdot \mu_r\left(\mathbf{B}(r,z,t)\right). \tag{4}$$

$$\gamma_\sigma(r,z,t) = \xi(z) \cdot \sigma. \tag{5}$$

where r and z are spatial coordinates of 2D axial symmetric model.

Numerical experiments revealed that if $\xi(z)$ function is continuous, the model is characterized by excellent convergence during solving, which was very important in our time-consuming simulations of the transient states in the coil modules. Function $\xi(z)$ employed in the description of the core dimensions and parameters of the applied ferromagnetic material was shown in Fig. 3.

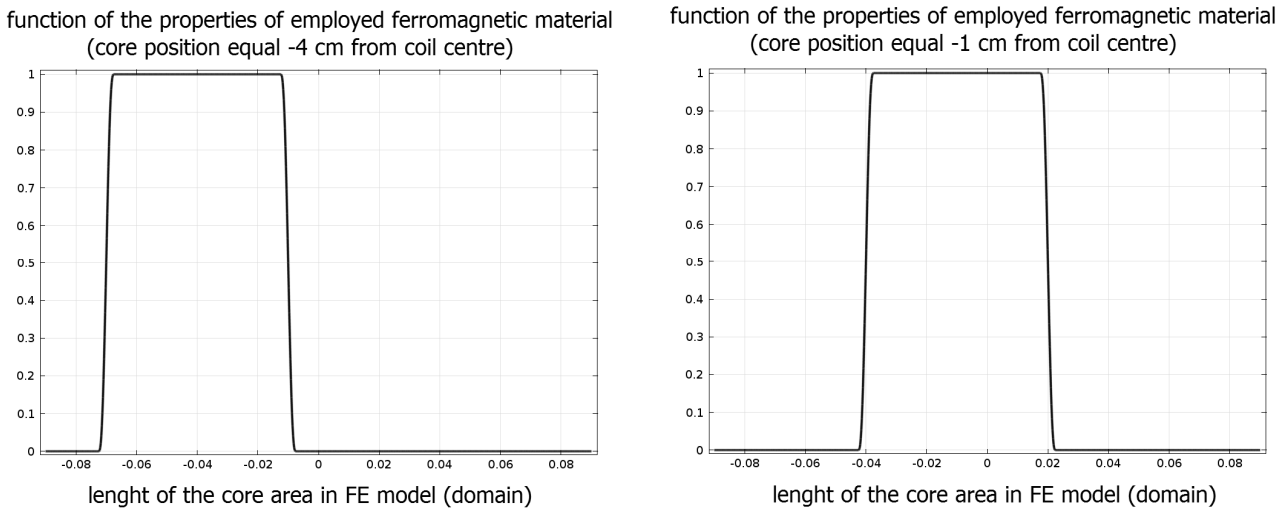

Fig. 3. Function $\xi(z)$ employed in the description of parameters ferromagnetic material

It should be underlined that the function $\xi(z)$ is independent of r coordinate because width of the core was limited by geometry drawn by means of COMSOL CAD module. This can be observed in Fig. 4.

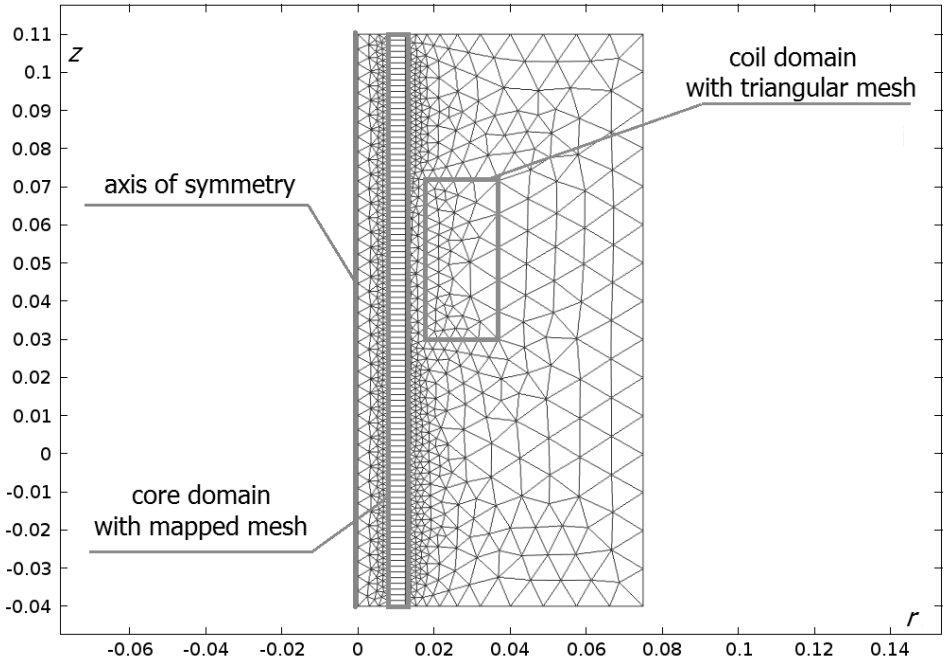

Fig. 4. Mesh of the FEM model which includes core motion described by the *Euler method*

The topology of the applied mesh was also crucial for model convergence and time of calculation. We decided to use a mapped mesh in the core domain and a triangular mesh in the remaining domains (coil and air). The mapped mesh was set as shown in Fig. 4. Its density was chosen with the usage of trial-and-error method.

Comparisons of the two above mentioned motion simulation methods showed that Euler's approach is way more efficient, less time-consuming and, at the same time, gives results similar to

those obtained with moving mesh method. The Euler's method enabled us to conduct time-dependent calculations involving core motion which we found the most useful and applied it to our numerical FEM model of single core-coil driving module. Result and additional description of that model can be found in our previous publications, for instance [3] and [7].

Field-circuit model of 10-coils launcher

Numerical model of the constructed device included mutual inductances between neighbouring coils. Our investigations concerning these lumped parameters, described in [7], indicated that in a single coil model only influence of the two closest solenoids is essential. In calculations which were carried out by means of FEM we took into consideration nonlinear ferromagnetic material (constructional steel). Numerical model was based on Ampere's Law for static and harmonic fields which were precisely described in our article, [7]. Introduction of harmonic perturbation was necessary to calculate self- and mutual inductances. We described the model of the investigated electromechanical coils-core system using above mentioned lumped parameters (self- and mutual inductances). It enabled us to connect field and circuit modelling approaches and derive simulation model of the entire launcher. Magnetic force acting on the core was used as an output from the electromagnetic part of the model. It was evaluated from FEM stationary model. Example of magnetic force distribution was depicted in Fig. 5.

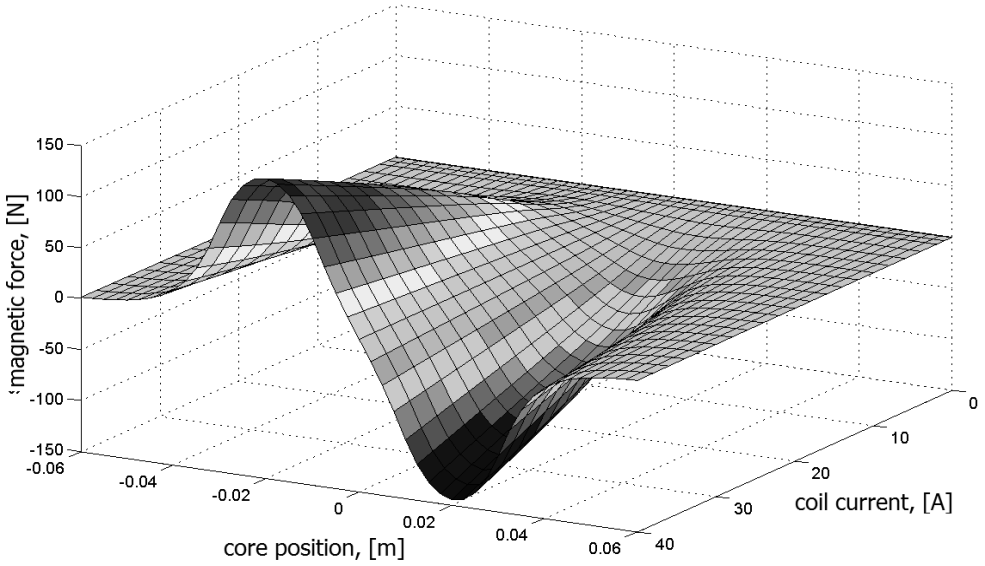

Fig. 5. Example of magnetic force distribution evaluated from FEM

Mechanical part of the field-circuit model of our launcher was described by Eq. 6 and schematically presented in Fig 6.

$$\frac{\mathrm{d}^2 z}{\mathrm{d}t^2} = \frac{F_m(z,i)}{\mathrm{m}} - \mathrm{g}\cdot\sin(\varphi) - \mu_\mathrm{C}\cdot\mathrm{g}\cdot\cos(\varphi)\cdot\mathrm{sign}\left(\frac{\mathrm{d}z}{\mathrm{d}t}\right) - \frac{\mathrm{b_v}}{\mathrm{m}}\cdot\frac{\mathrm{d}z}{\mathrm{d}t}. \tag{6}$$

where: z – position of the core (m), $F_m(z,i)$ – magnetic force computed by FEM as a function of core position (z) and coil current (i), [N]; g – gravitational constant, [m/s^2]; m – total mass of the moving parts applied to the launcher car (closest to the mass centre of all moving parts), [kg]; φ – launch angle, [deg]; μ_C – Coulomb friction coefficient, [dimensionless], b_v – viscous friction coefficient [N·s/m].

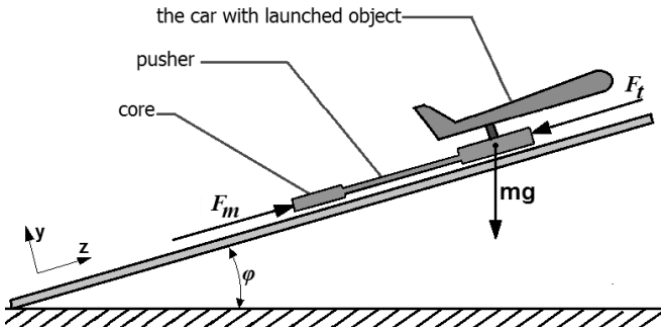

Fig. 6. Scheme of the mechanical part of the coil launcher model where F_t is friction force (N)

The derived numerical representation was used to develop and test control laws.

Control of the launch process

In order to control motion parameters during the launch we applied three control loops to each coil, where we introduced position, current, and acceleration sensors (Fig. 7).

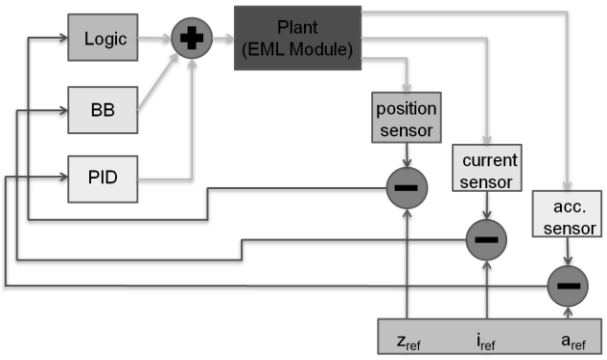

Fig. 7. Three control loops applied to each coil subsystem

Each logic loop was connected with the coils switching process. The particular solenoids were powered on and controlled when the core was approaching them and powered off with the core moving away from them. BB (*bang-bang*) loop was limiting current value in the coil circuit. The last loop (PID) was responsible for acceleration control. All 10 coils were controlled by one micro-controller which integrated sensors, executive transistor switches and control laws. As the platform for the control implementation we chose commercial board Arduino MEGA 2560.

Comparison of the launcher model with real-device characteristics

Signals from sensors mounted on the launcher were collected by Data Translation DT9804 card and filtrated by low pass filters. Bandwidths of filters were chosen experimentally. Additionally, we applied median filtration in order to minimize delays in position and acceleration signals. Using filtrated position signal we calculated velocity of the launched object. The main problem was connected with friction coefficients values. We proposed an algorithm, which during simulation, swept coefficients values and compared calculated signals of acceleration with the measured ones. The whole process, which was run offline, used already collected data. In order to find the best fit for μ_C and b_v the algorithm minimized the following equation:

$$J = \int_0^t (a_m - a_s)^2 \mathrm{d}t. \tag{7}$$

where: a_m - measured acceleration, [m/s^2] and a_s - simulated acceleration, [m/s^2].

Car braking phase was crucial for proper determination of the friction coefficients values. First, we tested the algorithm for 5-coil launcher due to the fact that braking process required a certain distance to stop the car. The number of coils used during the first tests was obtained by trial-and-error method. The results of fitting algorithm were shown in Fig. 8.

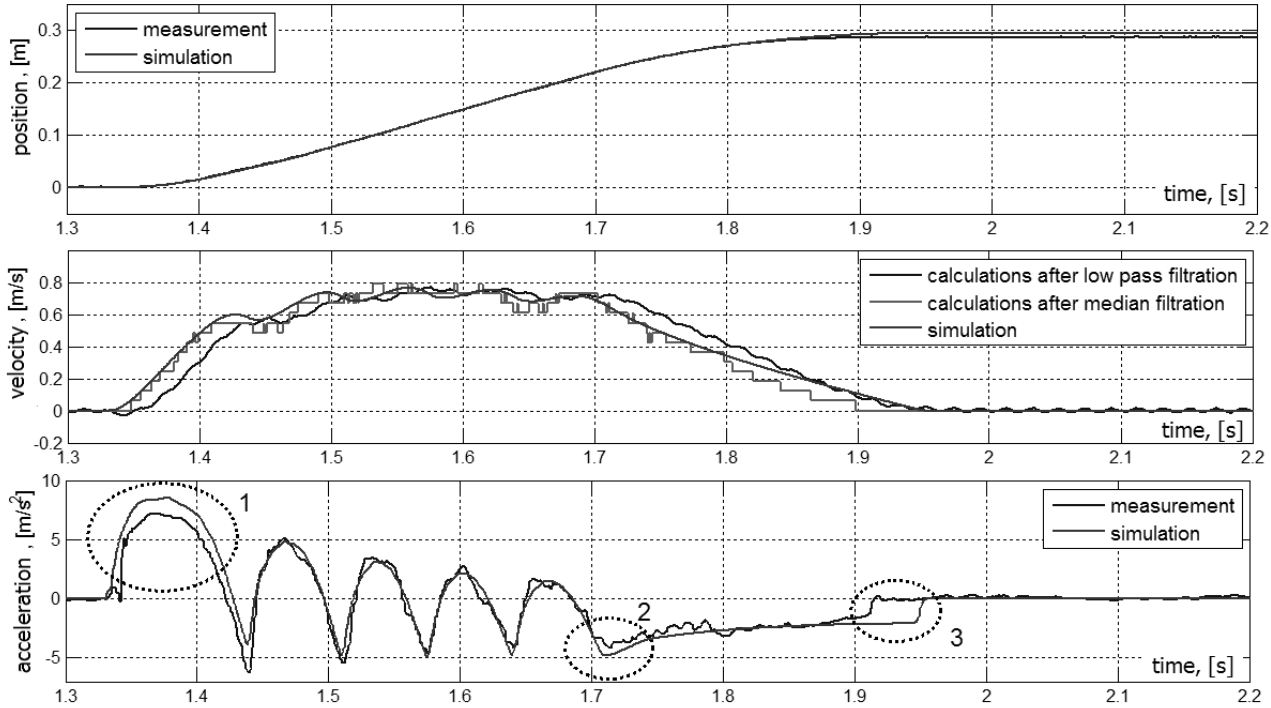

Fig. 8. Comparison of simulated and measured signals from designed EML, first tests were carried out for 5-coil launcher, velocity was calculated from position signal after low-pass and median filtration

In the diagram of acceleration signal (Fig. 8) we circled three areas where the simulation results significantly different from the measured data. During experiments we found out that this discrepancy was connected with rising coil resistance (area 1), lubrication introduced into construction (area 2) and with Stribeck friction effect which was not taken into account in the model (area 3).

Described algorithm was applied to position and acceleration signals measured during the tests on 10-coils launcher laboratory stand. Results of offline low-pass and median filtrations were presented in Fig. 9. It can be easily noticed that median filtration gave us less delays, especially in signal of estimated velocity. Moreover, implementation of median filters in a microcontroller systems is much simpler then low-pass and it works faster, which makes them applicable in real-time signal processing operations such as online filtration and rapid control. In our experiments velocity was calculated offline, because we just wanted to know how that signal evolved in time.

Comparison of the signals from 10-coils launcher and from numerical model were presented in Fig. 10. It is clearly visible that our numerical model corresponded to parameters of constructed launcher to a great extent. In the tests, we used control law in the form of simple switching sequence. Advanced control techniques will be researched soon and our results will be published in the next papers.

Conclusions

Presented approach for determining the friction coefficient values enabled us to construct the model of the 10 coil launcher which almost perfectly represent the real object and could be employed to developing and testing sophisticated control laws. Moreover, filtration system applied to collected data allowed us to estimate velocity of the launched objects. Constructed device and its numerical field-circuit model showed enormous research potential which will be developed in the future work.

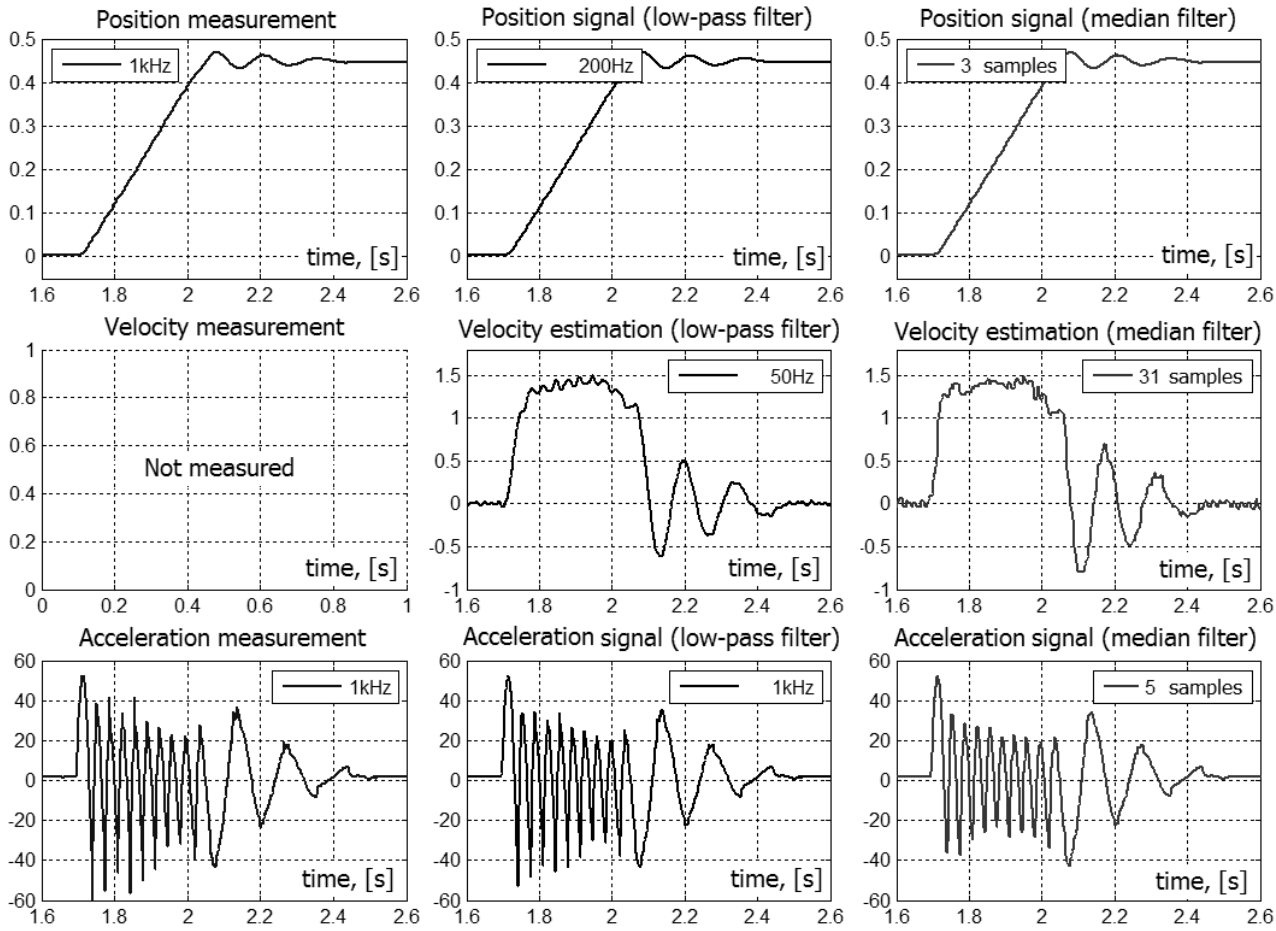

Fig. 9. Results of filtration performed on position and acceleration signals measured on 10-coils launcher laboratory stand. All quantities were presented in SI units.

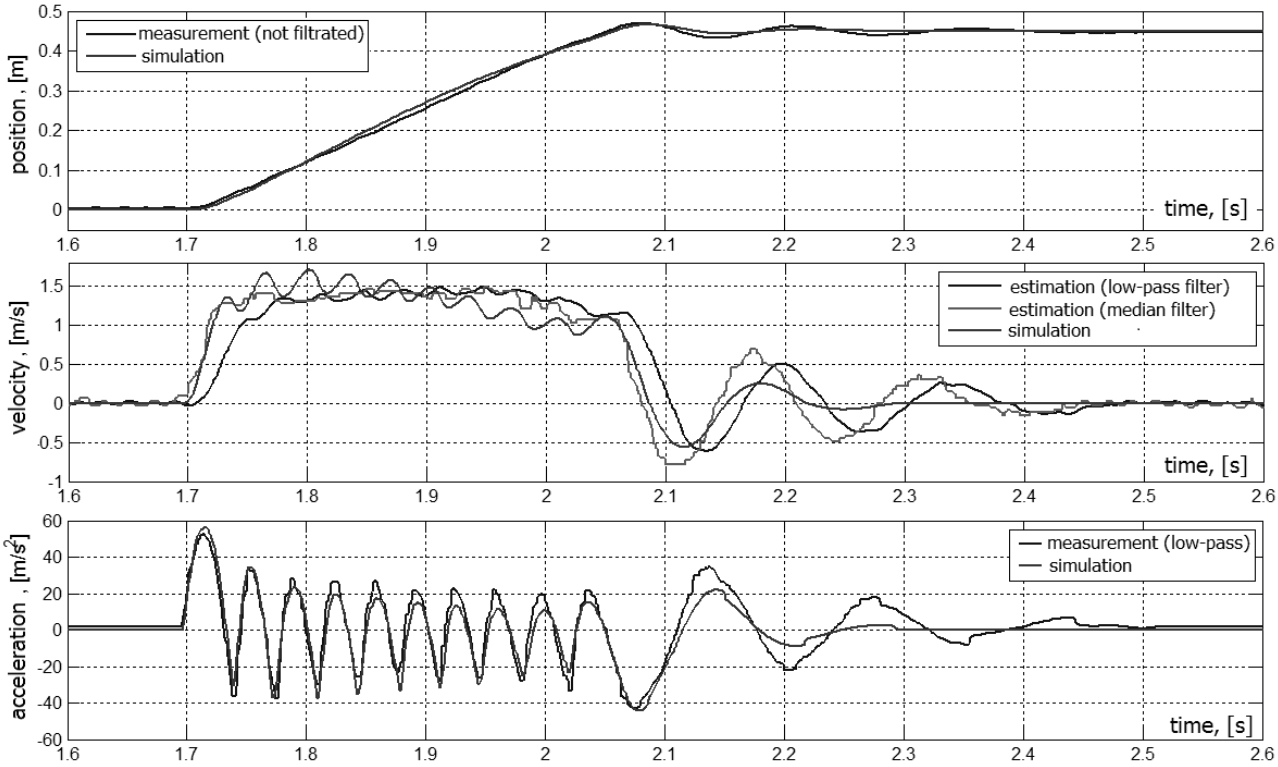

Fig. 10. Comparison of signals obtained from simulation and measured on 10-coils laboratory stand during tests

Acknowledgment

The research work is financed by Bialystok University of Technology as a research own work no. W/WM/11/2013.

References

[1] Z. Gosiewski, M. Kondratiuk: Introductory investigations of unmanned aerial vehicles (UAV) coil launcher, Scientific Proceedings of Riga Technical University, Series 6, Transport and Engineering. Transport. Aviation Transport, N27, Ryga, 2008.

[2] Gosiewski Z., Kondratiuk M.: Selection of Coils Parameters in Magnetic Launchers, Solid State Phenomena Vols. 147-149, 2009.

[3] Z. Gosiewski, M. Kondratiuk: Modelling of electromagnetic coil with mobile core for designing motion control in electromagnetic launchers, Transfer of Innovation to the Interdisciplinary Teaching of Mechatronics for an Advanced Technology Needs, Eds. E. Macha and G. Robak, Opole University of Technology, Opole, 2009.

[4] Z. Gosiewski, L. Ambroziak, Formation Flight Control Scheme for Unmanned Aerial Vehicles, Lecture Notes in Control and Information Science, vol. 422, pp. 331-340, Springer Verlag, 2012.

[5] L. Ambroziak, Z. Gosiewski, Preliminary UAV Autopilot Integration and In-Flight Testing, Solid State Phenomena, vol. 198, 2013, pp. 232-237.

[6] B. Tomczuk, A. Waindok: Linear Motors in Mechatronics – Achievements and Open Problems, Transfer of Innovation to the Interdisciplinary Teaching of Mechatronics for the Advanced Technology Needs, Opole University of Technology, Opole, 2009, pp. 358-377.

[7] B. Tomczuk, A. Waindok: A coupled field-circuit model of a 5-phase permanent magnet tubular linear motor, Archives of Electrical Engineering, Vol. 60, no. 1, 2011, pp. 5-14.

[8] A. Waindok, G. Mazur: Mutual Inductances in a Mathematical Model of the Three-Stage Reluctance Accelerator, 3rd International Students Conference on Electrodynamics and Mechatronics (SCE III), October 6-8, 2011, Opole, Poland, pp. 115-118.

[9] B. Reck, "First Design Study of an Electrical Catapult for Unmanned Air Vehicles in the Several Hundred Kilogram", IEEE Transaction on Magnetics, Vol. 3, No 1, pp. 15–64, 2003.

[10] W. Dengwu,L. Shaoke, L. Zhenxiang: Study of a Rail-Coil Hybrid Electromagnetic Launcher, Electrical Machines and Systems, 2008, pp. 944-947.

[11] M. Kondratiuk, Z. Gosiewski: Simulation Model of an Electromagnetic Multi-Coil Launcher for Micro Aerial Vehicles, Solid State Phenomena, Vol. 198, pp 406-411, Switzerland, 2013.

[12] M. Kondratiuk, Z. Gosiewski: Laboratory Stand of an Electromagnetic Multi-Coil Launcher for Micro Aerial Vehicles, Solid State Phenomena, Vol. 198, pp 334-339, Switzerland, 2013.

[13] J. F. Gieras, Z. J. Piech, B. Z. Tomczuk: Linear Synchronous Motors: Transportation and Automation Systems, 2nd Edition, Taylor & Francis, 2012.

[14] COMSOL Multiphysics, AC/DC Module User's Guide, COMSOL AB, October, 2011.